Boundary-Layer Meteorol (2007) 124:161–181
DOI 10.1007/s10546-007-9164-y

ORIGINAL PAPER

Influence of leaf water potential on diurnal changes in CO_2 and water vapour fluxes

Qiang Yu · Shouhua Xu · Jing Wang · Xuhui Lee

Received: 27 July 2006 / Accepted: 29 January 2007 / Published online: 15 March 2007

Abstract Mass and energy fluxes between the atmosphere and vegetation are driven by meteorological variables, and controlled by plant water status, which may change more markedly diurnally than soil water. We tested the hypothesis that integration of dynamic changes in leaf water potential may improve the simulation of CO_2 and water fluxes over a wheat canopy. Simulation of leaf water potential was integrated into a comprehensive model (the ChinaAgrosys) of heat, water and CO_2 fluxes and crop growth. Photosynthesis from individual leaves was integrated to the canopy by taking into consideration the attenuation of radiation when penetrating the canopy. Transpiration was calculated with the Shuttleworth-Wallace model in which canopy resistance was taken as a link between energy balance and physiological regulation. A revised version of the Ball-Woodrow-Berry stomatal model was applied to produce a new canopy resistance model, which was validated against measured CO_2 and water vapour fluxes over winter wheat fields in Yucheng (36°57′ N, 116°36′ E, 28 m above sea level) in the North China Plain during 1997, 2001 and 2004. Leaf water potential played an important role in causing stomatal conductance to fall at midday, which caused diurnal changes in photosynthesis and transpiration. Changes in soil water potential were less important. Inclusion of the dynamics of leaf water potential can improve the precision of the simulation of CO_2 and water vapour fluxes, especially in the afternoon under water stress conditions.

Keywords CO_2 flux · Leaf water potential · North China Plain · Water vapour flux · Winter wheat

Q. Yu (✉)· S. Xu · J. Wang
Institute of Geographical Sciences and Natural Resources Research,
Chinese Academy of Sciences, No. 11A, Datun Road, Beijing 100101, China
e-mail: yuq@igsnrr.ac.cn

X. Lee
School of Forestry and Environmental Studies, Yale University, New Haven, CT 06511, USA

1 Introduction

The CO_2 and water vapour fluxes to and from crop canopies are two important components of water-use efficiency when the soil respiration is relatively low. Therefore, their measurement and simulation are valuable for revealing mechanisms of mass and energy transfer and controls of crop productivity (Powell and Thorpe 1977; Chen and Coughenour 1994; Sellers et al. 1996; Baldocchi and Harley 1995; Wang and Leuning 1998). Many ecological models assume static plant conditions for which model parameters are not changed. For example, plant water status (leaf and xylem water potentials, water capacitance), the status of a photosynthetic system (maximum photosynthetic rate, P_{max}), initial photon yield (α), and the convex nature of the light response curve (β) are often held as constants through the day. Actually, these parameters change with time due to a cumulative effect of environmental variables on water balance and photosystem activity after sunrise (Yu et al. 2001).

Non-steady-state water transfer in the soil-plant-atmosphere continuum (SPAC) has been reported since the 1970s (Lhomme et al. 2001). Stomatal closure is stimulated by a leaf water potential decrease due to soil drying (Jensen et al. 2000), and it has been suggested that soil water deficit stimulates a root-shoot chemical signal, xylem borne abscisic acid (ABA), which is transported to the shoot and regulates the shoot physiological activity (Davies and Zhang 1991; Ali et al. 1998; Liu et al. 2005). Some methods have been developed to relate ABA synthesis rate in response to soil drying (Lhomme 2001). Moreover, a decline in soil and root hydraulic conductance due to soil drying may be an important control mechanism of stomatal closure (Yao et al. 2001), and there are several models that simulate water transport in the soil-root-canopy pathway (Grant 2001; Tuzet et al. 2003). However, Hirasawa and Hsiao (1999) found that on days of high vapour pressure deficit, leaf photosynthesis reached a maximum in the late morning and then decreased gradually as the day progressed, even though the soil was well irrigated. The midday reduction in stomatal conductance and photosynthesis was likely the result of low leaf water potential caused by high transpiration rates.

Plant water balance strongly influences turgor pressure of guard cells and, thereby, changes stomatal aperture. The same transpiration rate can correspond to two different water potentials indicating a change in plant water content (e.g., Kumagai 2001). Leaf water potential in the period of water loss is higher than in the period of water gain at a similar transpiration rate. Therefore, it is important to include changes in leaf water status for simulating changes in CO_2 and water vapour fluxes. This also provides a means of incorporating the effects of soil water stress on the CO_2 flux under different environmental conditions.

A change in leaf water potential controls stomatal aperture and, therefore, CO_2 and water fluxes (Jarvis and McNaughton 1986). In the Penman-Monteith (P–M) equation based on energy balance, canopy resistance to water vapour diffusion is the sole factor under physiological control (Thom 1975) and is a key point in the simulation of field evapotranspiration. As stomata are the main channels through which CO_2 uptake and water loss proceeds, there is a close relation among stomatal resistance and gas diffusion, photosynthesis, and transpiration (Goudriaan and van Laar 1978; Wong et al. 1979; Ball et al. 1987; Collatz et al. 1991; Leuning 1995; Yu and Wang 1998). The Ball-Woodrow-Berry (B-B) stomatal model has been used widely to evaluate plant productivity, biogeochemical cycling, and parameterization of land surface processes (Hatton et al. 1992; McMurtrie et al. 1992; Sellers et al. 1996;

Leuning et al. 1998; Yu and Wang 1998; Yu et al. 2001). From these relations at the leaf scale, canopy bulk stomatal resistance (canopy resistance) should be related to canopy photosynthesis and certain environmental factors in evapotranspiration models, such as the P–M equation.

The objectives of our study include, (1) to integrate a dynamic model of leaf water potential changes into the SPAC model (the ChinaAgrosys) of water and heat transfer and CO_2 assimilation, to distinguish the influence of water potential on CO_2 and water vapour fluxes over wheat; and (2) to calculate CO_2 and H_2O fluxes by scaling leaf photosynthesis and stomatal models up to the canopy level.

2 The model

The framework of the model ChinaAgrosys has been described by Wang et al. (2006, 2007), and includes leaf and canopy photosynthesis, a soil water dynamics and an evapotranspiration sub-models. The photosynthesis sub-model is a version of the simplified biochemical model of Farquhar et al. (1980), which combines the photosynthesis-stomatal conductance sub-model proposed by Collatz et al. (1991) with a version of the B-B model revised by Leuning (1995) and a newly proposed dynamic model of leaf water potential. Water vapour flux was simulated by the Shuttleworth-Wallace (S–W) equation in which the parameterization of canopy resistance was scaled from leaf stomatal up to the canopy.

2.1 Stomatal conductance

There is a close relationship between crop photosynthesis and stomatal conductance. Stomatal openings regulate photosynthesis by influencing the intercellular CO_2 concentration and, thereby, the biochemical processes in the chloroplast. The extent of stomatal opening is jointly determined by light intensity and water balance of guard cells. The former involves both the reaction of light receptors and the response to intercellular CO_2 concentration, and the latter is conditioned by the water balance of bulk leaf tissue and loss from the guard cells to the immediate aerial environment.

Ball et al. (1987) proposed a semi-empirical stomatal model in which stomatal conductance (g_s) was expressed by relative humidity or vapour pressure deficit (D) over a leaf surface, CO_2 concentration (C_s) and leaf photosynthetic rate (P_n) under conditions of ample water supply (Ball et al. 1987; Leuning 1995):

$$g_{\mathrm{s}} = \mathrm{m}\frac{P_{\mathrm{n}}}{(C_{\mathrm{s}} - \Gamma)(1 + D/\mathrm{D}_0)} + g_0. \tag{1}$$

The relation was revised by replacing relative humidity with leaf water potential (h_l) to include influences of both atmospheric water D and soil water (Tuzet et al. 2003):

$$g_{\mathrm{s}} = \mathrm{m}\frac{P_{\mathrm{n}}}{(C_{\mathrm{s}} - \Gamma)} f(h_{\mathrm{l}}) + g_0, \tag{2}$$

where Γ is the CO_2 compensation point, g_0 is cuticular conductance, and m is an empirical parameter. The function $f(h_{\mathrm{l}})$ is a correction factor, which ranges from 0 to 1. An empirical logistic function is used to describe the dependence of stomatal conductance on h_{l}:

$$f(h_l) = \frac{1 + \exp(s_l h_f)}{1 + \exp[s_l(h_f - h_l)]}, \tag{3}$$

in which h_f is a reference potential and s_l is a sensitivity parameter. The parameter values are adopted from Tuzet et al. (2003).

2.2 Canopy photosynthesis (P_{cg})

Light intensities within the canopy were calculated according to a negative exponential function with a canopy extinction coefficient (k) of 0.33. Canopy gross photosynthetic rate (P_{cg}) is integrated over the canopy using a leaf area index (L):

$$P_{cg} = \left(\frac{P_{max}}{k}\right) \ln\left(\frac{\alpha I + P_{max}}{\alpha I e^{-kL} + P_{max}}\right), \tag{4}$$

in which P_{max} is a function of temperature, h_l, and CO_2 concentration (Collatz et al. 1991; Yu et al. 2002).

2.3 CO_2 flux over the canopy (F_c)

F_c is estimated as the canopy net photosynthesis rate minus the sum of soil respiration (R_s), plant growth respiration (R_g) and maintenance respiration (R_m):

$$F_c = P_{cg} - (R_s + R_g + R_m). \tag{5}$$

Here, R_s is mainly a Q_{10} function of soil temperature modified by soil water content (Lee and Hu 2002):

$$R_s = R_0 \left(\frac{\theta}{a + \theta}\right)\left(\frac{b}{b + \theta}\right) Q_{10}^{(T_s - 25)/10}, \tag{6}$$

in which R_0 is the soil respiration at a reference temperature ($T_0 = 25°C$), θ is averaged soil water content in the root zone, a and b are regression coefficients, and Q_{10} is the ratio of the respiration rates over a 10°C temperature change.

R_m is a function of temperature and the total biomsass (B) of leaves, stems and roots. (Arora and Gajri 2000),

$$R_m = R_{m0} B Q_{10}^{(T_a - 20)/10} \tag{7}$$

where R_{m0} is a parameter representing maintenance respiration rates of leaves, stems and roots, which are set to 0.00125 kg kg^{-1} h^{-1}, 0.000625 kg kg^{-1} h^{-1} and 0.000417 kg kg^{-1} h^{-1} respectively.

Growth respiration of roots and shoots (R_g) is estimated as a constant fraction of gross photosynthetic rate (P_{cg}) minus maintenance respiration (Knorr 2000),

$$R_g = \begin{cases} r_g(P_{cg} - R_m), & P_{cg} - R_m > 0 \\ 0, & \text{otherwise} \end{cases} \tag{8}$$

where r_g is the growth respiration parameter.

2.4 Water movement in the soil

Soils were divided into n layers ($n \leqslant 10$) with variable depth, and the dynamic water movement was described by the Richards equation:

$$c(h_s, i)\frac{\partial h_s}{\partial t} = \frac{\partial}{\partial i}\left(K(h_s, i)\frac{\partial h_s}{\partial i}\right) - \frac{\partial K(h_s, i)}{\partial i} - S(i, t), \tag{9}$$

in which $c(h_s, i)$ is the specific water capacity of soil in the i^{th} layer, h_s is the soil water potential, $K(h_s, i)$ is the hydraulic conductivity of soil at h_s in the i^{th} layer, and $S(i, t)$ is the root uptake rate (Wang et al. 2006).

The rate of root water uptake rate at each layer can be represented as

$$S(i, t) = \frac{h_{\mathrm{s,i}} - h_{\mathrm{l}}}{r_{\mathrm{s,i}} + r_{\mathrm{r,i}} + r_{\mathrm{x,i}}}, \tag{10}$$

in which $r_{\mathrm{s,i}}$, $r_{\mathrm{r,i}}$ and $r_{\mathrm{x,i}}$ are the hydraulic resistances of the soil, the root radial resistance and root axial resistance at the i^{th} layer.

The hydraulic resistance of the soil is calculated according to single-root radial flow theory (Wang et al. 2002)

$$r_{\mathrm{s,i}} = \ln(b_i/a_r)/(2\pi K_i L_{d,i} D_i), \tag{11}$$

where a_{r} is the fine root radius, $L_{\mathrm{d,i}}$ is the root length density, and b_{i} is the path length for water uptake.

The root radial resistance is expressed as

$$r_{r,i} = r'_r/(L_{d,i} D_i), \tag{12}$$

where r'_r is the root radial resistivity.

The root xylem resistance is estimated from

$$r_{x,i} = r'_x z_{d,i}/(0.5 f L_{d,i}), \tag{13}$$

where r'_x is the root axial resistivity, $z_{\mathrm{d,i}}$ is the depth of the midpoint of the soil layer i, and f represents the fraction of the number of roots that connect to the shoot compared with the total number of roots.

2.5 Dynamics of leaf water potential

An effective water potential was considered for the big-leaf model. The leaf water status was determined by the balance between water loss through transpiration and supply from the soil through root absorption. Based on mass conservation, changes in plant water content are computed from water absorption and water loss:

$$c\frac{\mathrm{d}(\mathrm{h_s} - h_{\mathrm{l}})}{\mathrm{d}t} = T_{\mathrm{r}} - \frac{\mathrm{h_s} - h_{\mathrm{l}}}{R_{\mathrm{sl}}}, \tag{14}$$

where c is specific water capacitance, defined as the incremental changes in leaf water content (W) with h_{l} ($\mathrm{d}W/\mathrm{d}h_{\mathrm{l}}$), h_{s} is the average soil water potential in the root zone, h_{l} is the leaf water potential and R_{sl} is the resistance of water transfer from soil to leaf. The water potential of plants with lower water capacitance is more sensitive to changes in water content. R_{sl} will also change with soil and h_{l}. When soil becomes dry, transpiration decreases and water potential difference between soil and plant increases.

Therefore, the total resistance between roots and soil increases with decreased soil water potential (Cowan 1965).

Therefore, h_l is computed from

$$-c\frac{\mathrm{d}h_l}{\mathrm{d}t} = T_r - \frac{h_s - h_l}{R_{sl}}. \tag{15}$$

This equation was used to simulate the h_l based on the transpiration rate, and the h_l value then determined the stomatal conductance and transpiration. The relation was applied for single plants, and expressed per unit of ground area.

2.6 Evapotranspiration

The evapotranspiration was calculated according to the S–W equation, which separated soil evaporation and plant transpiration into two layers (Shuttleworth and Wallace 1985). Besides net radiation being partitioned betwen the soil and plant canopy, the key issue of the calculation is to parameterize a series of resistances for interfaces between soil, crop and atmosphere.

Aerodynamic resistance (r_a) under near-neutral conditions can be calculated form Thom (1975),

$$r_a = \ln^2[(z_r - d)/z_0]/(\kappa^2 u), \tag{16}$$

in which z_r is the reference height, u the wind speed, d the zero-plane displacement, and κ the von Karman constant; the empirical relations, $d = 0.67\,h_c$, and $z_0 = 0.12h_c$ are used, where h_c is crop height. For unstable conditions, r_a was modified according to Goudriaan (1977).

The crop canopy is usually assumed to be a random array of leaves in the big-leaf model, and the canopy resistance (r_c) consists of stomatal resistance of each layer in the canopy ($i = 1, \ldots, m$) ($r_{si} = 1/g_s$) (Lhomme 1991):

$$\frac{1}{r_c} = \sum_{i=1}^{m} \frac{1}{r_{si}}. \tag{17}$$

To scale up the stomatal model from leaf level (Eq. 1) to canopy level, the relationship between canopy resistance, canopy net photosynthesis (P_{cn}), atmospheric CO_2 (C_s) and h_l is given by:

$$\frac{1}{r_c} = a_1 \frac{P_{cn}}{(C_s - \Gamma)} f(h_l) + \frac{1}{r_{c0}}, \tag{18}$$

in which r_{c0} is cuticular resistance, and $1/r_{c0}$ is a summation of total g_0 for each leaf,

$$1/r_{c0} = Lg_0. \tag{19}$$

At the leaf scale, transpiration as well as photosynthetic rates can be simulated by a gaseous transfer equation as a function of environmental factors, in which physiological regulation of stomatal resistance is the key control. Evapotranspiration is evaluated on the basis of an energy balance at canopy scale, which also needs a canopy resistance scaled form leaf up to the canopy. Climate is the driving force of the gaseous fluxes. Parameters of plant physiology and soil physics are taken from experimental data or the literature (Table 2). The ChinaAgrosys model was driven by solar radiation, air temperature, humidity and wind speed at a reference height, as well as precipitation and irrigation. The leaf water potential sub-model was validated against

experimental data, in which plant water capacity is the dominating factor defining the amplitude of h_l in response to changing environmental variables. The value of P_{max} in the photosynthesis sub-model (Eq. 4) is an important factor in determining the CO_2 flux, and is of major concern in model calibration. The resistances of plant and soil play important roles in controlling water flow. The independent dataset was applied in model calibration. After initial values of soil temperature and water content are provided, the ChinaAgrosys model provides CO_2 and water fluxes, and soil water and temperature.

3 Numerical solution

In addition to the S–W equation and the photosynthesis sub-model, Eq. (1)–(19) are nonlinear and complete. Inputs to the ChinaAgrosys were microclimate and initial water content of the soil, and parameters reflecting the characteristics of crop physiological ecology. This set of equations was used to obtain the values of CO_2 and water vapour fluxes when environmental elements, i.e., solar radiation, air temperature, air vapour pressure, ambient CO_2, and wind speed or boundary-layer conductance, were provided as inputs (Fig. 1). The value of P_{cn} was obtained from the photosynthesis sub-model, and g_{sc} from Eq. 1. The h_l was dynamic, and Eq. 15 was first solved using the Runge-Kutta method. The initial h_l was set equal to soil water potential, and the transpiration rate was zero. After a series of resistances of water transfer were determined, the water vapour flux was calculated. Lastly, the water movement in the soil was computed from root absorption rate and soil evaporation.

The values of several parameters in the photosynthesis and stomatal conductance sub-models were taken from Collatz et al. (1991), Leuning (1995), and Yu et al. (2002). In the stomatal conductance sub-model, $m = 8$. Characteristic parameters of the h_l dynamics were determined according to validation and sensitivity analyses of h_l. Water capacitance was taken as $0.35 \times 10^{-8}\,m^3\,MPa^{-1}$, k_1 was 0.8 and R_{sl0} was $0.5 \times 10^7\,MPa\,s\,m^{-3}$. Most parameters in the ChinaAgrosys model are presented in Table 2. The model was calibrated against experimental data, with soil parameters derived based on the specific soil type and available measurements (Wang et al. 2006, 2007).

4 Site description and experiment

Observations were conducted in Yucheng Comprehensive Experimental Station (36°57′ N, 116°36′ E, 28 m above sea level) of the Chinese Academy of Sciences (a site of ChinaFlux, www.chinaflux.org) in 1997, 2001 and 2004. The site is located in the North China Plain, which is a large flat plain with a moderate monsoon climate. There was a fetch of more than 500 m for winds from all directions at each site. Meteorological variables, i.e. temperature, humidity, wind direction, wind speed and atmospheric pressure were measured with a temperature/humidity probe (HMP45C, Vaisala, Helsinki Finland), a potentiometer windvane (Model W200P, Vector, U.K.), an anemometer (A100R, Vector, U.K.), and a barometer (CS105, Vaisala, Finland). The total and net radiation data were collected using a pyranometer (CM11, Kipp&zonen, Canada) and a net four-component radiometer (CNR-1, Kipp&Zonen, Delft, The Netherlands). The instruments above were located at a height of 2.8 m above the ground.

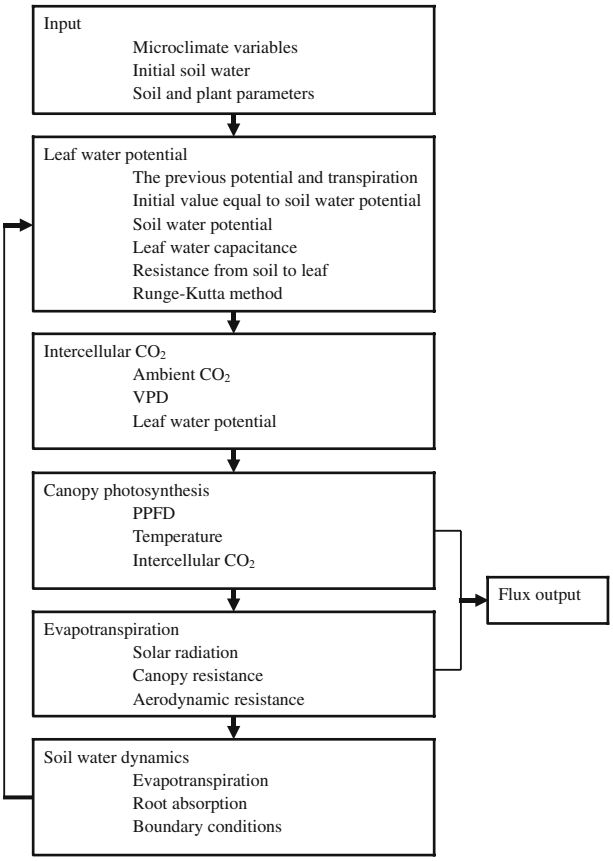

Fig. 1 Numerical solution of the model in simulation of CO_2 and water vapour fluxes

A three-dimensional sonic anemometer (Model CSAT3, Campbell Scientific, Inc., Logan UT) and an open path infrared gas analyzer (IRGA; Model LI-7500, LI-COR, Inc., Lincoln, NE) mounted at a height of 2.8 m measured the three components of the wind velocity, sonic temperature, and the densities of water vapour and CO_2. Soil heat flux was measured with a self-calibrating heat flux sensor (HFP01, Hukseflux, Netherlands) installed 0.05 m below the soil surface. The average values were calculated and recorded every 10 min. The area was occasionally irrigated as needed. The data were calibrated, and closure of the surface energy balance has been tested previously (Lee et al., 2004; Xiao et al. 2006; Wang et al. 2006).

Soil temperatures and water content were measured by four soil heat flux sensors (TCAV, Campbell Scientific, Logan, UT) installed at depths of 0.00, 0.10, 0.20 and 0.50 m and eight water content reflectometers (CS616_L, Campbell Scientific, Logan, UT) at depths of 0.00, 0.05, 0.10, 0.15, 0.20, 0.40, 0.60 and 1.00 m.

The variety of winter wheat was Zixuan 1. During the growing season, the leaf area index was measured every five days by harvesting 10 plants within a plot of 1 m^2, in which plants were counted. A trial of soil water stress was conducted in 2001, and there were 16 plots of 50 m^2. Soil water was controlled by sprinkling irrigation at

different frequencies and amount. Soil water stress was conducted under two conditions, i.e., light stress and strong stress. The diurnal variations of h_l were observed by the pressure chamber method according to Boyer (1995). Three wheat flag leaves were selected, and clipped to measure their water potentials.

5 Results

The results consist of the sensitivity analysis of the ChinaAgrosys model to solar radiation and soil water, the calibration of the leaf potential sub-model under consideration of lightly-stressed or strongly-stressed conditions, and the simulation of CO_2 and water vapour fluxes.

5.1 Analysis of model sensitivity

The model sensitivity to solar radiation and soil water was analyzed to demonstrate the performance of simulating the effect of h_l on CO_2 and water vapour fluxes. The simulation was performed with variable and constant h_l in Eq. 2. The difference may show the leaf water constraint. The ChinaAgrosys model was driven by solar radiation and air temperature, the initial value of h_l was set to the predawn soil water content (-1.0 MPa), and D increased exponentially with the temperature. Other input variables were also assumed constant during the day, i.e., wind speed was $1.5\,m\,s^{-1}$ and CO_2 concentration $360\mu mol\,mol^{-1}$. We used the method of changing one environmental factor or parameter at a time while holding others constant to observe the sensitivity of the ChinaAgrosys model. Photosynthesis and transpiration fluxes dominated over the soil fluxes for a closed canopy with $L = 3.5$. Their change in response to diurnal variations of environmental factors was analyzed.

5.1.1 Sensitivity of the model to solar radiation

The cumulative effect of water loss from the leaf caused h_l to reach its minimum in the afternoon, and to recover before sunset when solar radiation was low (Fig. 2). The photosynthesis under non-stressed conditions (when h_l was held constant) was higher than that under stressed conditions. This was evident under high solar radiation around noon, when h_l was at its minimum. Solar radiation was halved from Fig. 2 a2 to c2. Under higher solar radiation accompanied by strong water stress, photosynthesis was lower in the afternoon compared to the unstressed condition (Fig. 2). Diurnal changes in transpiration were similar to that of photosynthesis, but its midday depression was relatively small. The decrease in transpiration at midday was slight, because the decrease in g_s was compensated by the increase in D (Yu et al. 2001).

5.1.2 Sensitivity of the model to changes in soil water potential

Diurnal changes in h_l, see Fig. 3, showed photosynthesis and transpiration under slightly stressed and strongly stressed soil water conditions with soil water potentials set at -1.0, and -1.5 MPa, respectively. Photosynthesis was low under low soil water potential (i.e. low water content) in mid-afternoon but was not sensitive to different potential values in the morning. Transpiration decreased significantly with a decrease in soil water potential. Generally, transpiration increased with the water potential

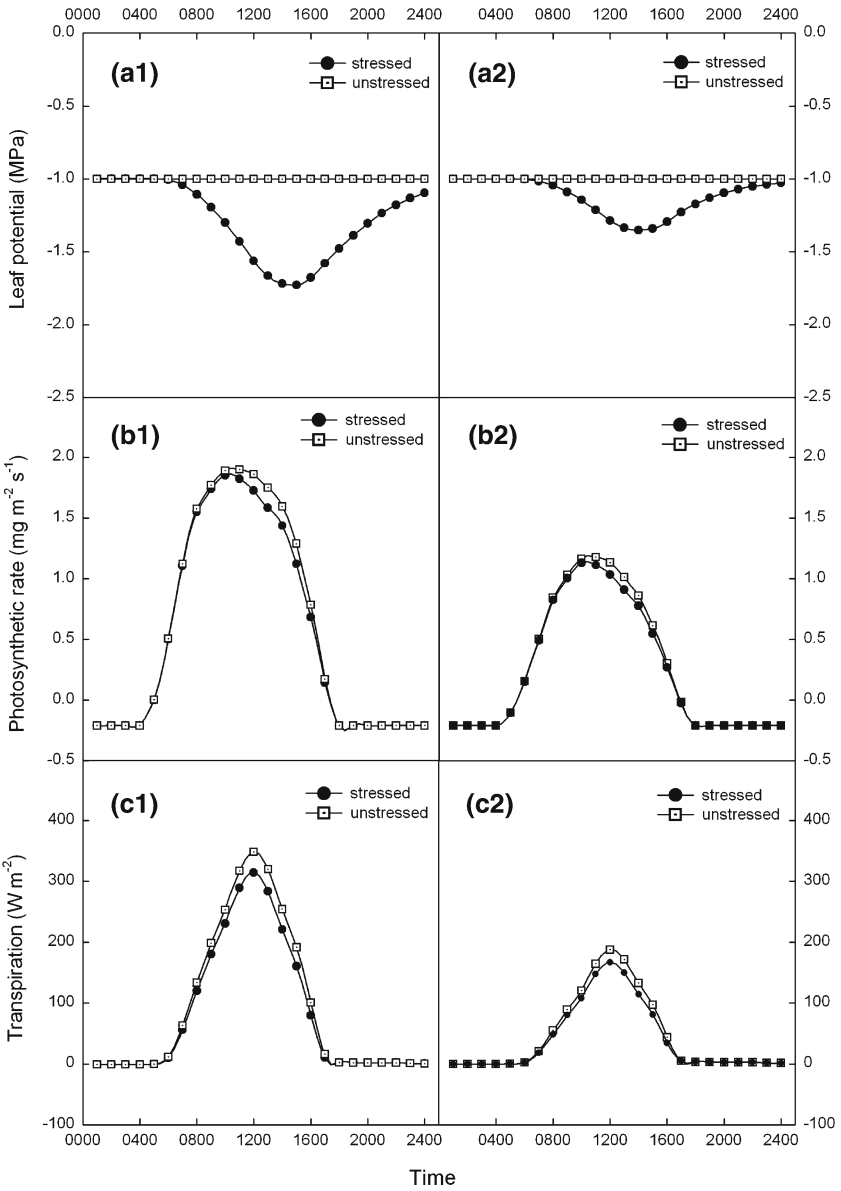

Fig. 2 Diurnal variations of leaf water potential, CO_2, and water vapour fluxes under normal meteorological conditions (left) and half of the solar radiation (right)

during daytime. Value of h_l decreased slowly in 3–4 h after sunrise and then decreased sharply with the increase in transpiration, and remained almost constant around noon. High light intensities caused high transpiration and loss of water, which decreased h_l. Leaf water potential recovered from its lowest value in the afternoon under strongly stressed conditions to reach the value found at night (Fig. 3). The sensitivity of the

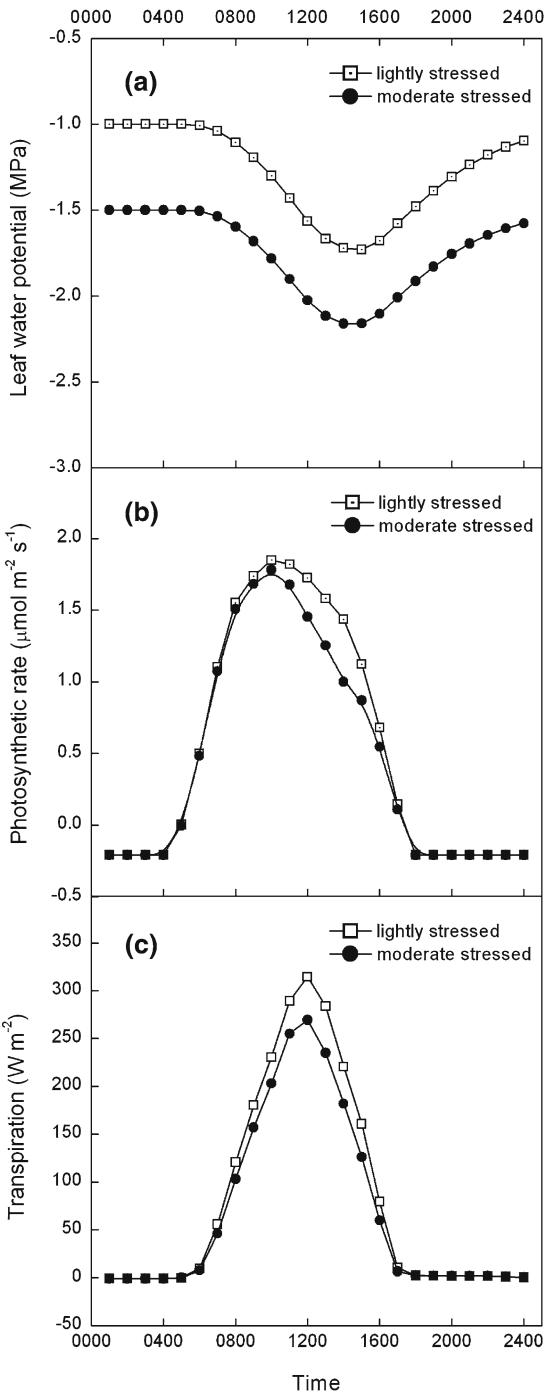

Fig. 3 Response of leaf water potentials and fluxes to different soil water potentials (−1.0 and −1.5 MPa)

analysis suggests that midday depression of photosynthesis may occur due to stomatal closure at low h_l.

5.2 Validation of the leaf water potential sub-model

The dynamics of leaf water potential is a key to the ChinaAgrosys model, and its validation determines the suitability of its incorporation with the photosynthesis and transpiration sub-models. The diurnal change in water potential of flag leaves and its simulation is shown in Fig. 4. The initial soil water potentials were −0.8, −1.1, and −1.1 MPa for April 26, May 12, and May 19, respectively. The root-mean-square error (RMSE) is $\sqrt{\frac{1}{n}\sum_{i=1}^{n}(Pi - Oi)^2}$, in which P and O are predicted and observed values, and n is the number of samples. The RMSE is 0.16 MPa for light stress, and 0.15 MPa for strong stress, indicating no significant difference in model error due to plant stress.

There was a close correspondence of trends in simulated and observed potentials. The lowest potential was achieved in afternoon around 1530 local time, which lagged 3.5 h behind the maximum solar radiation. The h_l recovered in the afternoon, along with a decrease in transpiration, and increased further during the night. The ChinaAgrosys model simulated h_l reasonably well under different soil water potential conditions (Fig. 4).

5.3 Validation of relationship between canopy resistance and photosynthesis

Canopy resistance was derived from the P–M equation under a closed canopy with $L = 2.3$ in the spring. Soil respiration was relatively small in the daytime. Canopy photosynthesis (P_{cn}) was subtracted from soil respiration, which was measured by the chamber method in this study area (Chen et al. 2004). Therefore, the relationship between canopy resistance and photosynthesis, D and CO_2 concentration was analysed (Fig. 5). It was shown that canopy resistance was closely related to canopy photosynthesis, as there was a significant diurnal variation.

5.4 Simulation of CO_2 and water vapour fluxes over wheat

CO_2 and water vapour fluxes were simulated according to experimental data reflecting the physiological characteristic and leaf photosynthetic observations (Yu et al. 2001, 2002). The fluxes were simulated by two methods. The first assumed constant h_l during the day corresponding to the pre-dawn h_l or soil water potential, while the other applied the dynamic equation of h_l.

The simulation with dynamic h_l was compared to constant h_l (Figs. 6 and 7). When dynamics in h_l were not considered, the simulated curves were higher than those for observations in the afternoon. The RMSE decreased from 0.31 to 0.20 mg m^2 s^{-1} for the CO_2 flux, and from 48 to 30 W m^{-2} for the water vapour flux after the variable h_l was simulated. This may be attributed to a decline in h_l after a period of illumination by solar radiation or water loss from plant leaves due to transpiration.

The trend of the simulated water vapour flux was smooth and agreed well with observations (Fig. 7). Generally, the simulated values were greater than the observed values if the decline of h_l in the afternoon was omitted. Once the water stress sub-model was used to simulate the changes in h_l, the flux corresponded to the observed value much better (Fig. 7). This improvement suggests that there is a midday

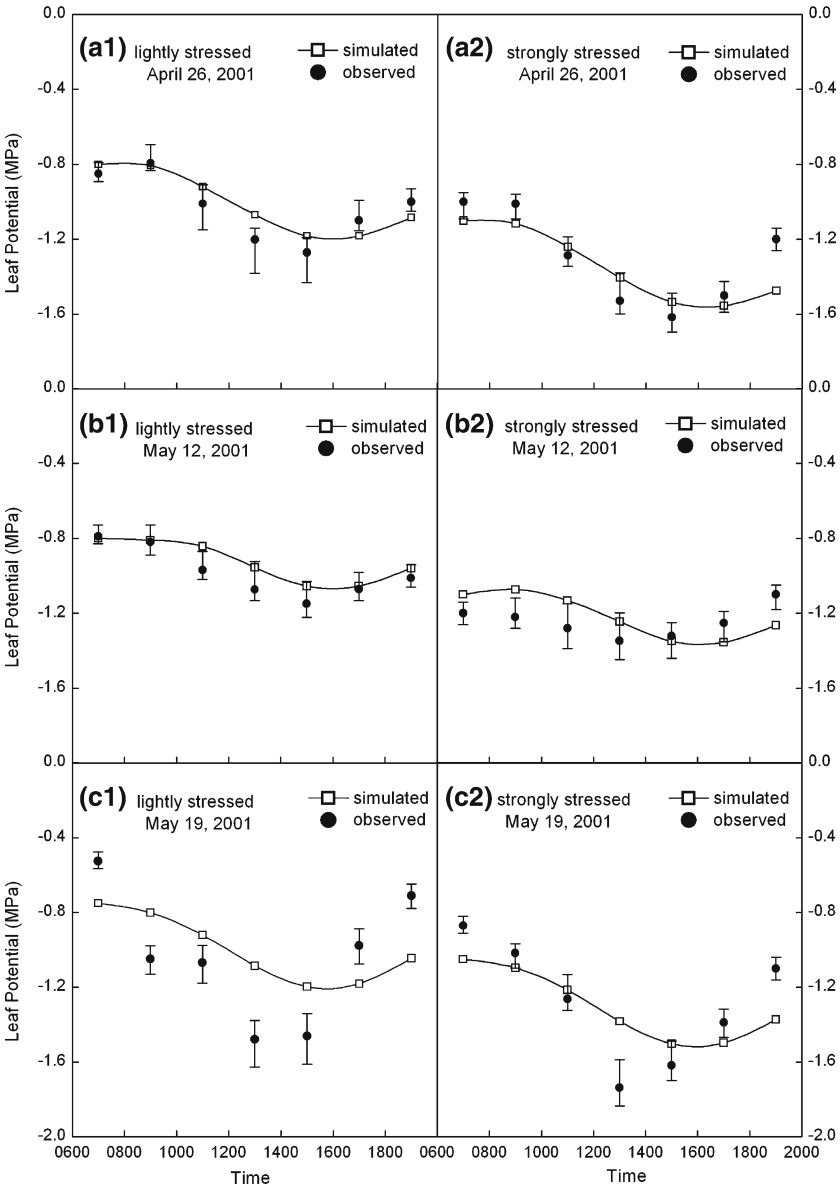

Fig. 4 Validation of leaf water potential model (26 April, 12 and 19 May, 2001)

depression of photosynthesis and transpiration that is influenced by stomatal control. Steady state crop status does not hold at a diurnal scale. The CO_2 and water vapour fluxes were simulated from turning-green to milking stages for wheat from March to May 2004. Figure 8 illustrates the flux simulation from shooting stage to grain filling stage with L from 2.2 to 5.8. The ChinaAgrosys model tracked the field measurements reasonably well: slopes were 0.97 and 0.96, and intercepts were 41 $W\,m^{-2}$ and 0.02 $mg\,m^{-2}\,s^{-1}$ respectively. The correlation coefficient (r) was 0.90 for both slope

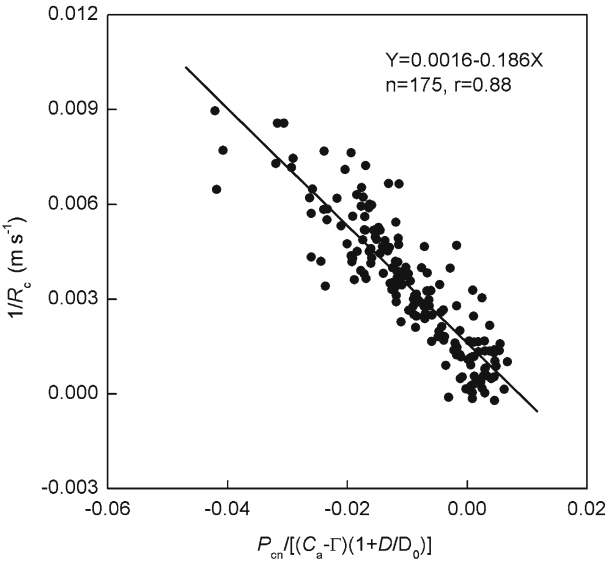

Fig. 5 Validation of canopy resistance model, i.e., Eq. 19, the relationship between canopy resistance and photosynthesis represented here by CO_2 flux (March 23–29, 2003)

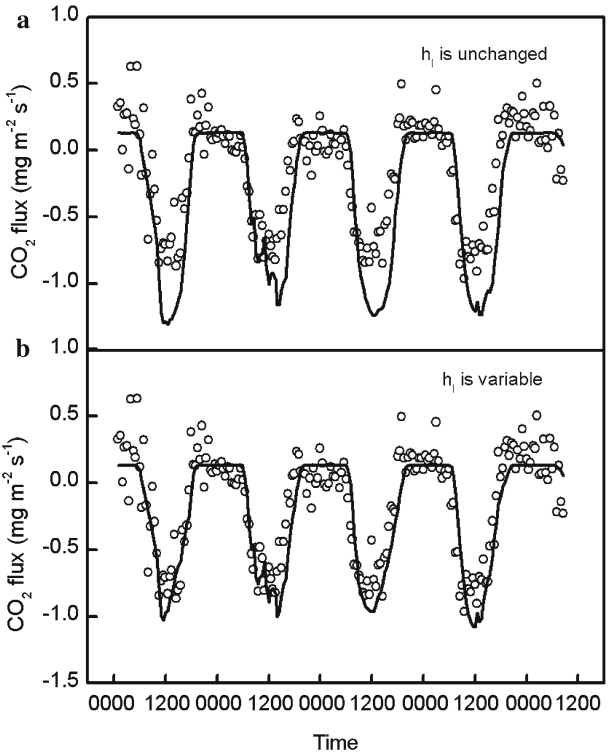

Fig. 6 Simulated and observed CO_2 fluxes (19–24 April, 2001), (**a**) and (**b**) are the simulations of CO_2 fluxes for unchanged h_l and variable h_l, respectively (initial soil water potential −1.1 MPa)

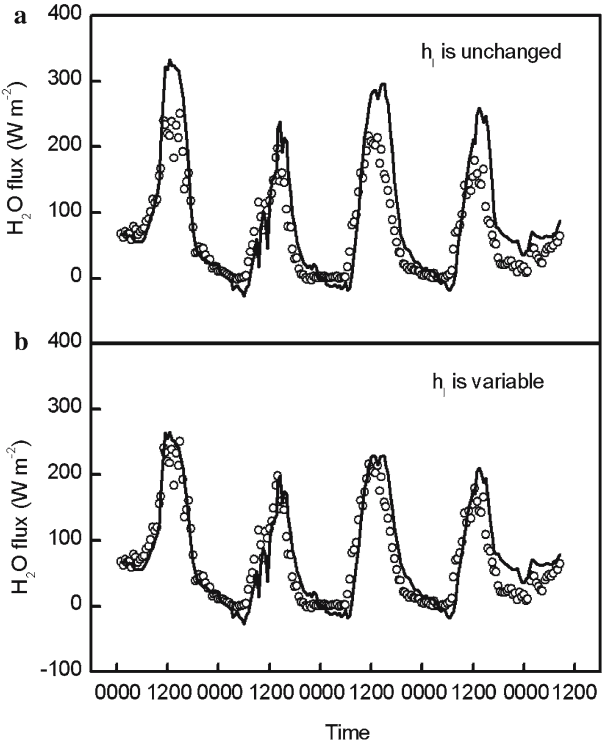

Fig. 7 Simulated and observed water vapour fluxes (19–24 April, 2001), (**a**) and (**b**) are the simulations of water vapour fluxes for unchanged h_l and variable h_l, respectively (initial soil water potential −1.1 MPa)

and intercept, and the RMSE values were 65 W m^{-2} and 0.22 mg m^{-2} s^{-1} for latent heat and CO_2 fluxes, respectively. Good predictions were obtained when changes in h_l were considered, indicating that the inclusion of leaf water control on photosynthesis and transpiration may increase simulation precision. Simulation of the fluxes showed higher discrepancy around noon if h_l was kept constant. The simulation can be improved by considering the influence of h_l on stomatal conductance and thereby the photosynthesis and transpiration rates.

Parameters in the ChinaAgrosys model were held constant in Fig. 8. The parameter V_m represents the assimilation of photosynthetic systems, which may differ among growth stages (Arora and Gajri 2000). It is determined by nitrogen content of leaf (Leuning 1995) and varies with development stages. But small changes in V_m can be assumed in the flourishing growth period during the period March 20–May 21 (Fig. 8).

6 Discussion

Root-zone soil moisture was included as a key variable controlling the surface water and energy balances (Albertson and Kiely 2001). There are some non-steady-state simulations of water transfer in plant canopies in the literature (Williams et al. 1996;

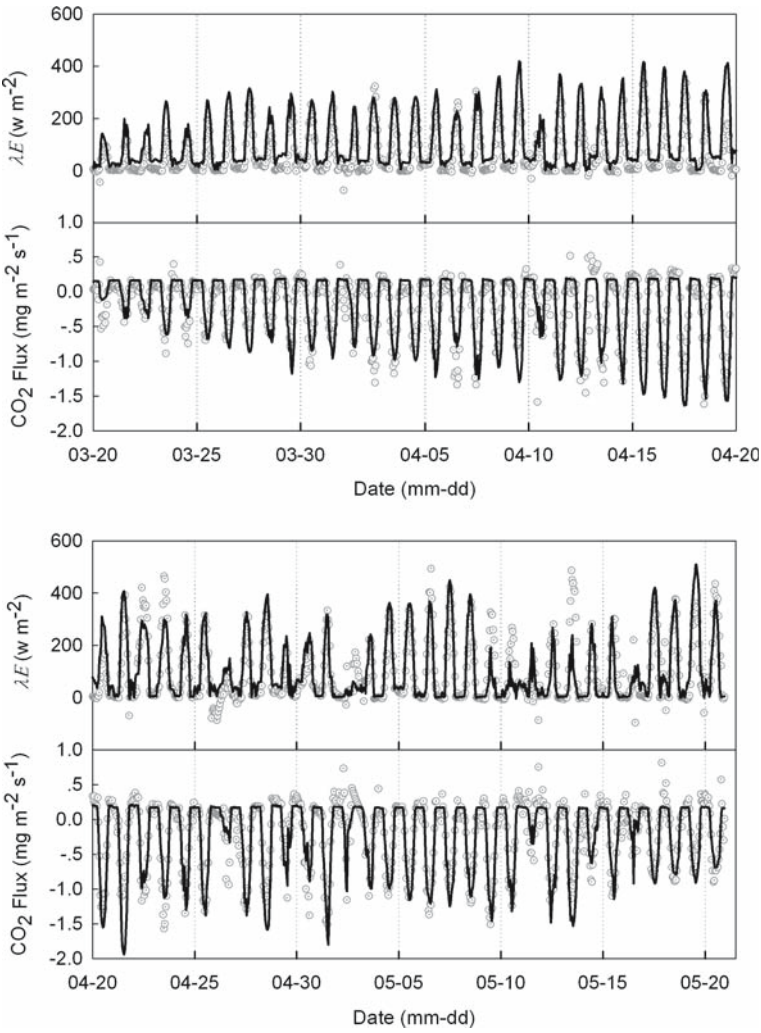

Fig. 8 Simulated and observed diurnal changes in CO_2 and water vapour fluxes (20 March–20 May, 2004). The leaf area index is 2.2–5.8, and the simulation was run by considering variable leaf water potential

Lhomme et al. 2001; Kumagai 2001) that describe dynamic changes in plant water content. Some of the plant and soil hydrological models include transpiration under changing h_l based on the water capacitance of leaves (Dauzat et al. 2001), but it is still a challenge to simulate the integrated response of h_l and transpiration with photosynthesis at the canopy scale. In the ChinaAgrosys, these relations were assimilated by scaling the stomatal model from the leaf up to the canopy (Eq. 19, Fig. 5). We considered canopy resistance (r_c) as a function of D, C_a and photosynthetic rate, which was integrated over L considering light extinction in the canopy. Some big-leaf models described r_c as a function of the mean leaf stomatal resistance (r_s) divided

by L ($\bar{r}_s/L$). This may lower prediction precision, because changes in r_c with L are nonlinear (Lhomme 1991).

Canopy photosynthesis and transpiration in physiological ecology and land surface processes should be scaled up from the leaf scale. One of the key problems in using the P–M or S–W equations is the parameterization of canopy resistance (Shuttleworth and Wallace 1985). Frequently, canopy resistance is calculated as a function of environmental elements, such as the 'Jarvis-type' model (1976). The empirical expression of r_c includes the multiplicative effect of influencing factors, but does not include the effects of physiological regulation and feedbacks. This implies that the Jarvis model may have less physiological reality than models of the B-B type (Eq. 1) based on physiological observations. The S–W equation separates the contributions of soil evaporation and plant transpiration to the water vapour flux. This is a convenient way of including the influence of changes in h_l on transpiration in the evapotranspiration prediction.

Models simulating water vapour and CO_2 fluxes were characterized by layered canopy and soil properties, parameterization of canopy resistance, and steady or non-steady status of h_l (Table 1). After a dynamic equation of h_l was combined in the ChinaAgrosys, feedbacks among h_l, stomatal conductance, intercellular CO_2 and photosynthetic rate were included. It may cause some error to use the big-leaf model, which simplifies light extinction, temperature, humidity and CO_2 profiles, and turbulence transfer within a canopy.

The core of the ChinaAgrosys model is Eq. 15, which describes the dynamics of water balance in a leaf. The introduction of Eq. 15 allows the model to simulate dynamic processes of h_l. Some other models (e.g. Choudhury and Monteith 1988; Chen and Coughenour 1994; Leuning et al. 1995; Sellers et al. 1996) contain constant parameters to simulate dynamic processes. An improved approach to simulation is to use a differential equation to include dependence on the plant status. Similar work has been done to describe the initial photon efficiency and to analyze diurnal changes in photosynthesis and transpiration (Yu et al. 2001). Also, Lakshmi and Wood (1998) simulated diurnal changes in evaporation using a two-layer hydrological model. This method of simulating dynamic processes generally interprets elements of the plant status and characteristics of the photosynthesis system (Yu et al. 2004).

Models describing fluxes through the interfaces in the system, which couple physical and physiological processes, are still at a semi-empirical stage. It is important to seek a balance of sub-models among processes. For example, we focused on the influence of h_l, and simply used the big-leaf model with the average radiation extinction coefficient for direct and diffuse radiation. As many models are 'plot-specific' (Goudriaan 1999), the process or factors that should be taken into consideration were identified by numerical analysis. For example, photosynthesis declined sharply in the afternoon, but simulation results showed smooth changes when h_l were held unchanged. The midday depression of photosynthesis may be ascribed to a decrease in stomatal opening and non-stomatal changes such as photoinhibition. When a plant is photoinhibited around midday, α decreases first, then P_{max}, and lastly β decreases (Demmig-Adams and Adams 1992; Long et al. 1994; Leverenz 1994). This study showed that the rate of CO_2 assimilation in leaves is depressed at moderate water deficits mostly as a consequence of stomatal closure (Chaves 1991). In fact, both stomatal and non-stomatal elements may be ascribed to midday depression of photosynthesis, which is a very common phenomenon under natural conditions (Xu and Shen 1997). Water deficits

Table 1 Comparison of process approaches used in models

Model	Canopy layers	Soil layers	Dynamics of plant status	Parameterization of canopy resistance
This study	Shuttleworth-Wallace evapotranspiration model and Exponential light extinction for photosynthesis	Multi-layers	Non-steady state	Related to canopy photosynthesis by scaling revised Ball-Berry (1987) model from leaf to canopy
Williams et al. (1996)	Multi-layers	Single layer	Non-steady state	Modified by meteorological variables
TWOLEAF Wang and Leuning (1998)	Sunlit and shaded two-leaves	Multi-layers	Steady state	Revised Ball-Berry model at leaf level
GEMTM Chen and Coughneour (1994)	Multi-layers	Multi-layers	Non-steady state	Ball-Berry model at leaf level
Lhomme et al. (2001)	Big-leaf	Single layer	Steady state	Jarvis-type formulation
Anderson et al. (2000)	Big-leaf	None	Steady state	Scaling Ball-Berry (1987) model from leaf to canopy, and photosynthesis is calculated by light use efficiency

may affect carbon assimilation through stomatal and non-stomatal processes. Stomatal conductance responds to air and soil humidity through leaf water status (feedback response) and direct response of stomata (feedforward response) (Lhomme 2001). Stomata can respond to soil water status independently of leaf water status. Soil drying stimulates a root-shoot chemical signalling, ABA in the xylem sap. Models have been developed to relate the ABA synthesis rate in response to soil drying (Lhomme 2001). At the next step, it is advisable to measure h_l and chloroplast fluorescence to distinguish the contribution of the stomatal and non-stomatal elements to the midday depression.

Physiological parameters in the ChinaAgrosys model may change with developmental stages, whereas the parameters used here were taken as constant, which may result in deviations from observations. Some observational days showed time changes in the simulated and observed fluxes that were similar in phase with different amplitudes. The water capacity may also vary with leaf water content, but there are many models that keep this constant, as a first-order approximation of the nonlinear relationship between water content and water potential (e.g., Wang et al. 2002).

Appendix

Table 2 Values of parameters and constants in the model

Parameter	value	Description and source
c	0.35×10^{-8} m^3 MPa^{-1}	Water capacitance (this study)
D_0	1.5 kPa	Parameter of humidity response (Leuning 1995)
κ	0.42	von Karman constant
m	8	Empirical parameter in Eq. 1 (Collatz et al. 1991)
Q_{10}	1.7	Arrhenus parameter for soil respiration (this study)
r_{c0}	1000 s m^{-1}	Residual resistance in Eq. 18 (this study)
R_0	0.11 mg m^{-2} s^{-1}	Soil respiration at reference temperature (25°C this study)
R_{m0}	0.677 g kg^{-1} h^{-1}	Maintenance respiration rate parameter (this study)
z_r	2.05 m	Reference height (this study)
a	0.001	Empirical parameter in Eq. 6 (Lee and Hu 2002)
b	3.82	Empirical parameter in Eq. 6 (Lee and Hu 2002)
S_l	5	Empirical parameter in Eq. 3 (This study)
h_f	−2 MPa	Reference leaf water potential in Eq. 3 (this study)
a_r	0.002 m	Empirical parameter in Eq. 11 (Wang et al. 2002)
r'_r	4.9×10^{11} s m^{-1}	Empirical parameter in Eq. 12 (Wang et al. 2002)
r'_x	3.5×10^{10} s m^{-3}	Empirical parameter in Eq. 13 (Wang et al. 2002)
f	0.22	Empirical parameter in Eq. 13 (Wang et al. 2002)
r_g	0.35	Growth respiration parameter in Eq. 8 (Knorr 2000)

Acknowledgements Two anonymous reviewers are gratefully acknowledged for their valuable suggestions and comments. We thank Dr. Tim Green in USDA-ARS for his review of the manuscript. This work is supported by National Natural Science Foundation of China (No. 40328001) and Chinese Academy of Sciences International Partnership Project "Human Activities and Ecosystem Changes" (No. CXTD-Z2005-1).

References

Albertson JD, Kiely G (2001) On the structure of soil moisture time series in the context of land surface models. J Hydrol 243:101–119

Ali M, Jensen CR, Mogensen VO (1998) Early signals in fieldgrown wheat in response to shallow soil drying. Aust J Plant Physiol 25:871–882

Anderson MC, Norman JM, Meyers TP, Diak GR (2000) An analytical model for estimating canopy transpiration and carbon assimilation fluxes based on canopy light-use efficiency. Agric For Meteorol 101:265–289

Arora VK, Gajri PR (2000) Assessment of a crop growth-water balance model for predicting maize growth and yield in a subtropical environment. Agric For Meteorol 46:157–166

Baldocchi DD, Harley PC (1995) Scaling carbon dioxide and water vapour exchange from leaf canopy in a deciduous forest II: model testing and application. Plant Cell Environ 18:1157–1173

Ball JT, Woodrow IE, Berry JA (1987) A model predicting stomatal conductance and its contribution to the control of photosynthesis under different environmental conditions. In: Biggins I (ed) Progress in photosynthesis research Martinus Nijhoff Publishers, The Netherlands, pp 221–224

Boyer JS (1995) Measuring the water status of plants and soils. Academic Press, New York, pp 33–45

Chaves MM (1991) Effects of water deficits on carbon assimilation. J Exp Bot 42:1–16

Chen SY, Li J, Lu PL (2004) Soil respiration characteristics in winter wheat field in North China Plain. Chin J Appl Ecol 15:1552–1560 (in Chinese with English abstract)

Chen DX, Coughenour MB (1994) GEMTM: a general model for energy and mass transfer of land surfaces and its application at the FIFE sites. Agric For Meteorol 68:145–171

Choudhury BJ, Monteith JL (1988) A four-layer model for heat budget of homogeneous land surfaces. Quart J Roy Meteorol Soc 114:373–398

Collatz GJ, Ball JT, Grivet C, Berry JA (1991) Physiological and environmental regulation of stomatal conductance photosynthesis and transpiration: a model that includes a laminar boundary layer. Agric For Meteorol 54:107–136
Cowan IR (1965) Transport of water in the soil–plant–atmosphere system. J Appl Ecol 2:221–239
Dauzat J, Rapidel B, Berger A (2001) Simulation of leaf transpiration and sap flow in virtual plants: model description and application to a coffee plantation in Costa Rica. Agric For Meteorol 109: 143–160
Davies WJ, Zhang J (1991) Root signals and the regulation of growth and development of plants in drying soil. Annu Rev Plant Physiol Plant Molec Biol 42:55–76
Demmig-Adams B, Adams WW III (1992) Photoprotection and other responses of plants to high light stress. Annu Rev Plant Physiol Plant Molec Biol 43:599–626
Farquhar GD, von Caemmerer S, Berry JA (1980) A biochemical model of photosynthetic CO_2 assimilation in leaves of C_3 species. Planta 149:78–90
Goudriaan J, van Laar HH (1978) Relations between leaf resistance CO_2- concentration and CO_2 assimilation in maize beans lalang grass and sunflower. Photosynthetica 12:241–249
Goudriaan J (1977) Crop micrometeorology: a simulation study. In: Simulation monographs. Center for Agricultural Publishing and Documentation, Wageningen, The Netherlands, 249 pp
Goudriaan J (1999) Predicting crop yield under global change In: Walker B, Steffen W, Canadell J et al (eds) The terrestrial biosphere and global change. Cambridge University Press, U.K., pp 106–140
Grant RF (2001) A review of the Canadian ecosystem model ecosys In: Shaffer M (ed) Modeling carbon and nitrogen dynamics for soil management. CRC Press, Boca Raton, FL, pp 175–264
Hatton TJ, Walker J, Dawes WR, Dunin FX (1992) Simulations of hydroecological responses to elevated CO_2 at the catchment scale. Austral J Bot 40:679–696
Hirasawa T, Hsiao TC (1999) Some characteristics of reduced leaf photosynthesis at midday in maize growing in the field. Field Crops Res 62:53–62
Jarvis PG (1976) The interpretation of the variations in water potential and stomatal conductance found in canopies in the field. Phil Trans Roy Soc London Ser B 273:593–610
Jarvis PJ, McNaughton KG (1986) Stomatal control of transpiration: scaling up from leaf to region. In: MacJadyen A, Ford RD (eds) Advances in ecological research, vol 15. Academic Press, London pp 205–265
Jensen CR, Jacobsen SE, Andersen MN, Núñez N, Andersen SD, Rasmussen L, Mogensen VO (2000) Leaf gas exchange and water relation characteristics of field quinoa (Chenopodium quinoa Willd) during soil drying. Eur J Agron 13:11–25
Knorr W (2000) Annual and interannual CO_2 exchanges of the terrestrial biosphere: process based simulations and uncertainties. Biogeography 9:225–252
Kumagai T (2001) Modelling water transportation and storage in sapwood-model development and validation. Agric For Meteorol 109:105–115
Lakshmi V, Wood EF (1998) Diurnal cycles of evaporation using a two-layer hydrological model. J Hydrol 204:37–51
Lee XH, Hu XZ (2002) Forest-air fluxes of carbon water and energy over non-flat terrain. Boundary-Layer Meteorol 103:277–301
Lee XH, Yu Q, Sun XM, Liu JD, Min QW, Liu YF, Zhang XZ (2004) Micrometeorological fluxes under the influence of regional and local advection: a revisit. Agric For Meteorol 122:111–124
Leuning R, Dunin EX, Wang YP (1998) A two-leaf model for canopy conductance photosynthesis and partitioning of available energy II Comparison with measurements. Agric For Meteorol 91:113–125
Leuning R, Kelliher FM, De Pury DGG, Schulze ED (1995) Leaf nitrogen photosynthesis conductance and transpiration: scaling from leaves to canopies. Plant Cell Environ 18:1183–1200
Leuning R (1995) A critical appraisal of a combined stomatal-photosynthesis model for C_3 plants. Plant Cell Environ 18:339–355
Leverenz JW (1994) Factors determining the nature of the light dosage response curve of leaves In: Baker NR, Bowyer JR (eds) Photoinhibition of photosynthesis from molecular mechanisms to the field BIOS. Scientific Publishers, Oxford, pp 239–254
Lhomme JP, Rocheteau A, Ourcival JM, Rambal S (2001) Non-steady-state modelling of water transfer in a Mediterranean evergreen canopy. Agric For Meteorol 108:7–83
Lhomme JP (1991) The concept of canopy resistance(historical survey and comparison of different approaches. Agric For Meteorol 54:227–240
Lhomme JP (2001) Stomatal control of transpiration: examination of the Jarvis-type representation of canopy resistance in relation to humidity. Water Resour Res 37:689–699

Liu FL, Andersen MN, Jacobsen SE, Jensen CR (2005) Stomatal control and water use efficiency of soybean (*Glycine max* (L.) Merr.) during progressive soil drying. Environ Exp Bot 54:33–40

Long SP, Humphries S, Falkowski PG (1994) Photoinhibition of photosynthesis in nature. Annu Rev Plant Physiol Molec Biol 45:633–662

McMurtrie RE, Leuning R, Thompson WA, Wheeler AM (1992) A model of canopy photosynthesis and water use incorporating a mechanistic formulation of leaf CO_2 exchange. For Ecol Manage 52:261–278

Powell DB, Thorpe B (1977) Dynamic aspects of plant-water relations in environmental effects on crop physiology. Academic Press, London, pp 159–279

Sellers P J, Randall DA, Collatz GJ, Berry JA, Field CB, Dazlich DA, Zhang C, Collelo GD, Bounoua L (1996) A revised land surface parameterization (SiB2) for atmospheric GCMs Part I: model formulation. J Climate 9:676–705

Shuttleworth WJ, Wallace JS (1985) Evaporation from sparse crops-an energy combination theory. Quart J Roy Meteorol Soc 111:839–855

Thom AS (1975) Momentum mass and heat exchange of plant communities. In: Monteith JL (ed) Vegetation and the atmosphere, vol. 1. Principles, Academic Press, London, pp 57–109

Tuzet A, Perrier A, Leuning R (2003) Stomatal control of photosynthesis and transpiration: Results from a soil–plant–atmosphere continuum model. Plant Cell and Environ 6:1097–1116

Wang J, Yu Q, Lee XH (2007) Simulation of crop growth and energy and carbon dioxide fluxes at different time steps from hourly to daily. Hydrol Process 21:

Wang S, Grant R, Verseghy D, Black TA (2002) Modelling carbon-coupled energy and water dynamics of a boreal aspen forest in a general circulation model land surface scheme. Int J Climatol 22:1249–1265

Wang J, Yu Q, Li J, Li LH, Li XG, Sun XM, Yu GR (2006) Simulation of diurnal variations of CO_2 water and heat fluxes over winter wheat with a model coupled photosynthesis and transpiration. Agric For Meteorol 137:194–219

Wang YP, Leuning R (1998) A two-leaf model for canopy conductance photosynthesis and partitioning of available energy I: model description and comparison with a multi-layered model. Agric For Meteorol 91:89–111

Williams M, Rastetter EB, Fernandes DN, Goulden ML, Wofsy SC, Shaver GR, Melillo JM, Munger JW, Fan SM, Nadelhoffer KJ (1996) Modelling the soil–plant–atmosphere continuum in a Quercus-Acer stand at Harvard Forest: the regulation of stomatal conductance by light nitrogen and soil/plant hydraulic properties. Plant Cell Environ 19:911–927

Wong SC, Cowan IR, Farquhar GD (1979) Stomatal conductance correlates with photosynthetic capacity. Nature 282:424–426

Xiao W, Yu Q, Flerchinger GR, Zheng YF (2006) Evaluation of SHAW model in simulating energy balance leaf temperature and micrometeorological variables within a maize canopy. Agron J 98: 722–729

Xu DQ, Shen YG (1997) Midday depression of photosynthesis. In: Pessarakli M (ed) Handbook of Photosynthesis. Marcel Dekker pp 451–459

Yao C, Moreshet S, Aloni B (2001) Water relations and hydraulic control of stomatal behaviour in bell pepper plant in partial soil drying. Plant Cell Environ 24:227–235

Yu Q, Wang TD (1998) Simulation of the physiological responses of C_3 plant leaves to environmental factors by a model which combines stomatal conductance photosynthesis and transpiration. Acta Bot Sin 40:740–754

Yu Q, Goudriaan J, Wang TD (2001) Modeling diurnal courses of photosynthesis and transpiration of leaves on the bases of stomatal and non-stomatal responses including photoinhibition. Photosynthetica 39:43–51

Yu Q, Liu YF, Liu JD, Wang TD (2002) Simulation of leaf photosynthesis of winter wheat on Tibetan Plateau and in North China plain. Ecol Model 155:205–216

Yu Q, Zhang YQ, Liu YF, Shi PL (2004) Simulation of the stomatal conductance of winter wheat in response to light temperature and CO_2 changes. Ann Bot 93:435–441